

Evidence for an Anderson transition in granular Sn films

C. Van Haesendonck* and Y. Bruynseraede

Laboratorium voor Vaste Stof-Fysica en Magnetisme, Katholieke Universiteit Leuven, B-3030 Leuven, Belgium

(Received 14 February 1985; revised manuscript received 4 October 1985)

Conductivity and density-of-states measurements have been performed on granular Sn films with room-temperature conductivities $\sigma(300\text{ K})$ between 1 and $10^4\ \Omega^{-1}\text{ cm}^{-1}$. Our conductivity measurements indicate that superconductivity as well as normal metallic behavior disappear at the metal-insulator transition ($\sigma_c \approx 40\ \Omega^{-1}\text{ cm}^{-1}$). The anomalous magnetoconductivity in the metallic phase is consistent with the scaling picture for the Anderson transition. The temperature dependence of the conductivity is more complex, probably due to the influence of the granular film structure. The importance of the enhanced Coulomb repulsion near the Anderson transition is directly reflected by the appearance of a square-root anomaly in the density of states around the Fermi level. The granularity of the Sn films causes this anomaly to be considerably smaller than for homogeneous amorphous metals.

I. INTRODUCTION

Recently, the nature of the metal-insulator transition and the possible existence of a minimum metallic conductivity¹ have attracted much renewed interest.² Many new results on a wide variety of disordered systems illustrate the importance of electron localization³ and Coulomb correlations.⁴ It is now generally accepted that the Anderson transition⁵ induced by increasing disorder is continuous. Experimentally, the macroscopic conductivity σ_∞ disappears continuously when the conductivity σ_0 on a microscopic scale L_0 reaches the critical value σ_c :

$$\sigma_c \approx A \frac{e^2}{\hbar L_0}. \tag{1}$$

For noninteracting electrons Mott¹ estimated $A \approx 0.025$.

McMillan⁶ extended the scaling approach to the Anderson transition to take into account the Coulomb repulsion between the conduction electrons. Since the long-range Coulomb repulsion is strongly enhanced by the reduced diffusivity, electron correlations will increase the σ_c value and $A \approx 0.1$. For homogeneous amorphous mixtures, L_0 corresponds to the interatomic distance. Equation (1) predicts a σ_c value of the order of $500\ \Omega^{-1}\text{ cm}^{-1}$. This is in good agreement with the experimental results obtained for amorphous Nb-Si (Ref. 7) and Au-Ge (Ref. 8) mixtures. Due to the Coulomb correlations, the density of states N will also become scale dependent in the metallic phase. The relevant length scale L is determined by the temperature T or the energy separation $|E - E_F|$ from the Fermi level:

$$L(T, E) = \left[\frac{\xi^2 \Delta}{\max(k_B T, |E - E_F|)} \right]^{1/2}. \tag{2}$$

ξ is the correlation length which diverges at the Anderson transition, while the characteristic energy scale Δ goes to zero when the Anderson transition is approached. It should be noted that Eq. (2) is only valid in the macro-

scopic metallic limit ($\xi < L, \Delta > |E - E_F|$).

The validity of McMillan's phenomenological scaling approach can be checked directly by measuring the temperature dependence of the conductivity. McMillan showed that for the macroscopic metallic limit, this temperature dependence is given by

$$\begin{aligned} \sigma(T) &= \frac{\sigma_c L_0}{\xi} \left[1 + \frac{\xi}{L(T)} \right] \\ &= \sigma_\infty \left[1 + \left(\frac{k_B T}{\Delta} \right)^{1/2} \right]. \end{aligned} \tag{3}$$

Experimentally, the σ_∞ value can be obtained by extrapolating the temperature dependence of the conductivity towards $T=0$: $\sigma_\infty = \sigma(T \rightarrow 0)$. On the other hand, the energy dependence of the density of states is given by

$$\begin{aligned} N(|E - E_F|) &= N(L_0) \left[\frac{L_0}{\xi} \right]^{3-\eta} \left[1 + \frac{\xi}{L(|E - E_F|)} \right] \\ &= N(E_F) \left[1 + \left(\frac{|E - E_F|}{\Delta} \right)^{1/2} \right]. \end{aligned} \tag{4}$$

Although McMillan failed to use the thermodynamic density of states to describe the screening of the Coulomb repulsion, Eqs. (3) and (4) provide an excellent fit for $\sigma(T)$ and $N(E - E_F)$ measurements in amorphous Nb-Si mixtures. The square-root anomaly in the density of states of granular Al films⁹ can also be described by Eq. (4). Due to the presence of superconductivity at lower temperatures and the complex temperature dependence of the conductivity above the superconducting transition, no attempt was made to compare the results for $\sigma(T)$ and $N(E - E_F)$.

In this paper we compare quantitatively the square-root anomaly in the density of states and the temperature dependence of the conductivity for a disordered granular material. We report on our measurements of $\sigma(T)$ and

$N(E - E_F)$ in metallic and insulating granular Sn films [$1 \Omega^{-1} \text{cm}^{-1} < \sigma(300 \text{ K}) < 10^4 \Omega^{-1} \text{cm}^{-1}$]. As we will show, McMillan's scaling theory can explain qualitatively the basic features of the metal-insulator transition in granular Sn films. Consistency between the conductivity and density-of-states measurements can, however, only be obtained when the inhomogeneous structure of the granular Sn is taken into account.

In granular superconductors, the $\sigma(T)$ variation can be studied in a broader temperature range, when the superconductivity is destroyed by a large magnetic field. In granular Al,¹⁰ $\sigma(T) \propto T^{1/2}$ even for $B \sim 10 \text{ T}$. The $T^{1/2}$ dependence can be explained by short-range Coulomb correlations (neglected in McMillan's calculation) that are still present at high magnetic fields. The localization correction to the conductivity is completely destroyed by the field, since the relevant length scale L_B defined as

$$L_B = \left[\frac{\hbar}{eB} \right]^{1/2} \quad (5)$$

is much smaller than the correlation length ξ . At lower fields, where ξ and L_B are comparable, there appears a positive magnetoconductivity in the granular Al films which is given for $T \rightarrow 0$ by the empirical formula:¹¹

$$\frac{\sigma(B)}{\sigma(B=0)} = C \left[1 + \frac{\xi}{L_B} \right], \quad (6)$$

where $C \simeq 1$ is a constant. One expects therefore a magnetic field dependence $\sigma(B) - \sigma(B=0) \propto B^{1/2}$. Equation (6) has been verified experimentally for granular Al.¹¹ For granular Sn we also observe a $B^{1/2}$ dependence, but the constant C in Eq. (6) is negative (negative magnetoconductivity). This experimental observation can be explained by assuming the presence of a strong spin-orbit scattering in our granular Sn films. Although no detailed calculation has been performed, one expects that C has to be replaced by $-C/2$ in Eq. (6) when the spin-orbit scattering becomes strong.

The $T^{1/2}$ dependence of the conductivity is no longer observed for granular Al films that are close to the Anderson transition.¹⁰ In these films, the superconductivity is substantially suppressed by the localization, leading to a reduction of the transition temperature T_c . Although these films do not show the characteristic activated electronic transport of the insulating phase, the $\sigma(T)$ variation is faster than a power law of T . It is not clear whether $\sigma(T \rightarrow 0)$ in these films is still nonzero. If $\sigma(T \rightarrow 0) = 0$, one could consider the possibility of a superconducting ground state existing in the insulating phase. On the other hand, the anomaly in the density of states for granular Al films close to the Anderson transition is still described by Eq. (4), indicating a metallic behavior.⁹ As will be shown, the experimental situation in our granular Sn films is very similar. For homogeneous, amorphous Nb-Si mixtures⁷ $\sigma(T) \propto T^{1/2}$ even for films that are very close to the Anderson transition. We therefore will link the complex $\sigma(T)$ variation in our Sn films to the inhomogeneous, granular structure.

A granular material consists of metallic grains coated by a highly resistive oxide, so that the electronic conduc-

tion will be extremely inhomogeneous on an atomic length scale. Hence, it is rather surprising that Eq. (4), which was obtained for homogeneous amorphous materials, can also be used to describe the density of states for granular Al. As pointed out by Imry,¹² the results of the scaling theory remain valid if the microscopic properties are calculated on a length scale $L_0 = L_g$, where L_g is the average grain size. In this way, the influence of the insulating coating is taken into account since the material properties are homogeneous on a scale $L \gg L_g$. An important consequence of this redefinition of L_0 is the decrease of σ_c as compared to the value for a homogeneous, amorphous metal. For a typical grain size $L_g = 10 \text{ nm}$, Eq. (1) predicts $\sigma_c \simeq 20 \Omega^{-1} \text{cm}^{-1}$. Experimentally, one indeed finds such a small value for σ_c in granular metals.¹³

The electron localization and the enhanced Coulomb repulsion in disordered conductors also strongly influence the superconducting properties.¹⁴ For homogeneous amorphous mixtures, the alloying of a superconducting metal with a nonmetal will change the superconducting properties when the Anderson transition is approached. It is therefore very difficult to check the possible universal destruction of superconductivity by Anderson localization in these materials. In Nb-Si mixtures, e.g., superconductivity disappears completely before the Anderson transition is reached.⁷

In a granular metal superconductivity is destroyed when the superconducting phase coherence between the metal grains is destroyed by critical fluctuations and charging effects in the grains. Incorporating the granular properties into the scaling theory for the metal-insulator transition, Imry and Strongin¹⁵ showed that superconductivity completely disappears (also in the individual grains) when $\sigma_0 = \sigma_c$, provided that the grain size L_g is small ($L_g \leq 5 \text{ nm}$). For larger grain sizes, the individual grains may still be superconducting in the insulating phase ($\sigma_0 < \sigma_c$), while conduction in the normal state is only possible via thermally activated hopping. At very low temperatures, the grains are coupled coherently by the Josephson effect and superconductivity appears on a macroscopic scale. It should be noted that the approach of Imry and Strongin completely neglects the influence of percolation upon the metal-insulator transition. When the grain size and the thickness of the insulating coating vary, percolation can become very important.

The paper is organized as follows. In Sec. II we describe the preparation and characterization of the granular Sn films. In Sec. III we discuss the conductivity and density of states in the framework of the theoretical models.

II. EXPERIMENT

The granular Sn films are prepared by evaporating pure Sn (99.999%, Balzers) in a reduced oxygen atmosphere onto a glass substrate held at room temperature. The film thickness t checked with a crystal-oscillator thickness monitor was for all Sn films of the order of 100 nm. By keeping the oxygen pressure constant at approximately $5 \times 10^{-2} \text{ Pa}$ and changing the deposition rate, films could be obtained with a conductivity ranging between $\sigma(300 \text{ K}) = 10^4 \Omega^{-1} \text{cm}^{-1}$ (films show a metallic behavior and a

very sharp superconducting transition at $T_c \simeq 3.75$ K) and $\sigma(300 \text{ K}) = 1 \Omega^{-1} \text{ cm}^{-1}$ (films are insulating and show no sign of superconductivity). Previous studies clearly indicated that Sn films prepared under these conditions are granular.¹⁶ The average grain size for granular Sn is larger than for granular Al films. Since the grain size distribution is also broader for granular Sn, this implies that the inhomogeneous film structure will have a stronger influence on the Anderson localization. The inhomogeneous structure of our Sn films is also confirmed by the experimental fact that the “macroscopic” mean free path $l_{el}(d)$ obtained from the film thickness and the film resistance at $T = 4.2$ K (assuming for Sn the free electron value $\rho l_{el} = 4.7 \times 10^{-12} \Omega \text{ cm}^2$) can become much smaller than the interatomic spacing. The poor conductivity on a macroscopic scale at low temperatures can be explained by the reduced probability for tunneling through the insulating coating of the grains. On the other hand, the mean free path $l_{el}(\mathcal{R})$ obtained from the resistance ratio $\mathcal{R} = R(300 \text{ K})/R(4.2 \text{ K})$ (we take $\rho = 11.3 \mu\Omega \text{ cm}$ for the resistivity due to electron-phonon scattering at $T = 300$ K), is much larger than $l_{el}(d)$, indicating that there still exists a good metallic conduction within the Sn grains.

The composition of the granular Sn films was analyzed by ion-scattering spectroscopy (ISS). From these measurements we conclude the following:

(i) The oxygen is homogeneously distributed throughout the film. We therefore may assume that there are no macroscopic inhomogeneities (≥ 100 nm) present in the film which may cause experimental deviations from the scaling theory for the Anderson transition.

(ii) The oxygen concentration in the vicinity of the metal-insulator transition is considerably smaller than the amount needed to form a stable film of SnO or SnO₂. The dominant elastic scattering at the amorphous oxide layers coating the Sn grains will cause an Anderson transition to the insulating phase.

We also prepared tunnel junctions of the cross-strip geometry, where the granular Sn film served as the top electrode. The base electrode was either a pure Sn or a pure Al film on which a native oxide was grown to form the tunneling barrier. The square tunneling area was defined using a photoresist layer so that edge effects could be avoided. From the tunneling results we obtain direct information about the superconducting and normal density of states of the granular Sn films. In this way, the influence of electron-electron interactions on the metal-insulator transition are studied.

With use of a conventional ⁴He cryostat and a superconducting magnet, the films and the junctions were measured in the temperature range $1 < T < 20$ K and in magnetic fields up to $B = 4$ T. We also took care to keep the measuring voltages low enough to avoid non-Ohmic behavior due to the heating of the granular Sn films.

III. RESULTS AND DISCUSSION

The conductivity measurements as a function of temperature indicate that a metal-insulator transition occurs when $\sigma(300 \text{ K})$ has reached the critical value $\sigma_c \simeq 40 \Omega^{-1} \text{ cm}^{-1}$. In the vicinity of the transition, the tempera-

ture dependence of σ around $T = 300$ K is much weaker than at low temperatures. If the large $\sigma(T)$ variations at low temperatures are due to Anderson localization, this indicates that the relevant length scale $L(300 \text{ K})$ is comparable to the grain size L_g . We therefore assume that $\sigma(300 \text{ K})$ gives a good estimate of the disorder on a microscopic scale and that the metal-insulator transition occurs when $\sigma(300 \text{ K}) \simeq \sigma_0 = \sigma_c \simeq 40 \Omega^{-1} \text{ cm}^{-1}$. From Eq. (1) we estimate that the average grain size L_g is of the order of 5 nm. Although we did not perform transmission electron microscopy on our Sn films, we note that this grain size is comparable to the value $L_g \simeq 3$ nm reported for granular Al films near the metal-insulator transition.¹⁷

As predicted by the scaling theory [see Eq. (3)], the influence of the Anderson transition is already observable in the metallic state. Figure 1 shows a typical result for a metallic Sn film with $\sigma_0 \simeq \sigma(300 \text{ K}) = 67 \Omega^{-1} \text{ cm}^{-1}$. We observe an anomalous increase of the resistivity $\rho = \sigma^{-1}$ with decreasing temperature. The increase is faster than logarithmic (see dashed line) and the resistivity change is considerably larger than expected for a weakly localized two-dimensional film. This is in agreement with the fact that due to the significant elastic scattering, the Sn film ($t \simeq 100$ nm) will behave as a three-dimensional disordered metal.

The sharp decrease of the resistivity around $T = 3$ K (see Fig. 1) is due to the superconducting transition in the granular Sn film. The Anderson localization reduces the

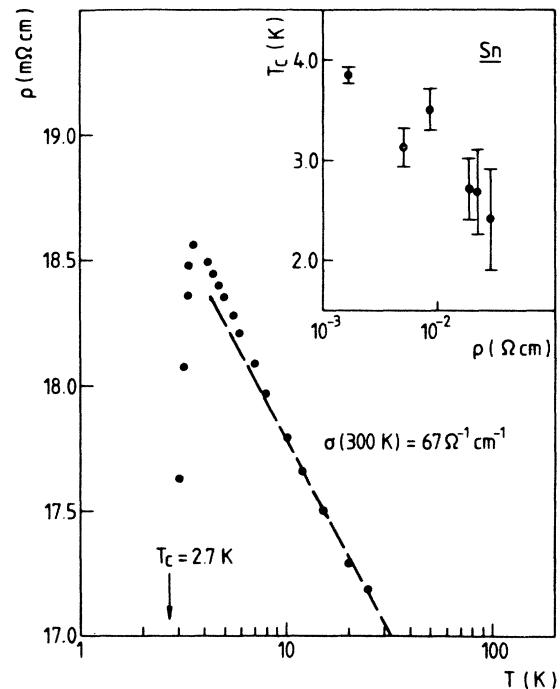


FIG. 1. Variation of the resistivity as a function of temperature (logarithmic scale) for a granular Sn film with a superconducting transition at 2.7 K. The dashed line represents the linear variation expected for a weakly localized two-dimensional metal. The inset shows the depression of the superconducting transition temperature T_c with increasing resistivity $\rho(4.2 \text{ K})$. The error bars represent the width of the transition.

T_c value in the metallic regime. This decrease of T_c with increasing resistivity $\rho(4.2\text{ K})$ is shown in the inset of Fig. 1. It should be noted that a similar decrease was also observed in granular Al films.^{9,17} The error bars represent the broadening of the superconducting transition which can be explained by the large critical fluctuations in individual Sn grains.¹⁷

The most important conclusion we draw from our $\sigma(T)$ measurements is the complete destruction of superconductivity when the insulating phase is reached [$\sigma(300\text{ K}) \simeq 40\ \Omega^{-1}\text{cm}^{-1}$]. This is illustrated in Fig. 2 for a Sn film with $\sigma(300\text{ K}) = 36\ \Omega^{-1}\text{cm}^{-1}$. Electronic conduction is only possible via thermally activated hopping. The linear decrease of $\ln(\sigma)$ as a function of $T^{-1/4}$ indicates that variable range hopping is the dominant electronic transport process.¹ Over the whole temperature range ($1.5 < T < 25\text{ K}$), there appears no irregularity which might be connected to the presence of superconductivity in the individual Sn grains. Using the theory of Imry and Strongin for the destruction of superconductivity in granular metals, this indicates that the average grain size L_g is rather small ($L_g \leq 5\text{ nm}$), which is in agreement with the grain size obtained from the σ_c value.

It is obvious that the presence of superconductivity in the granular Sn films (see Fig. 1), hinders a detailed analysis of the metallic conductivity using Eq. (3). Previous experiments⁷ showed that such an analysis is only possible at very low temperatures ($T \leq 1\text{ K}$). This is consistent with McMillan's scaling approach since the macroscopic metallic regime is only reached when $\Delta \gg k_B T$ [see Eq. (2)]. As for the case of granular Al,¹⁰ we find that the $\sigma(T)$ variation in the normal state is becoming considerably faster than a power law of T for metallic samples near the metal-insulator transition [$\sigma(300\text{ K}) \leq 150\ \Omega^{-1}\text{cm}^{-1}$]. When a high magnetic field is applied, superconductivity is no longer present on a macroscopic scale. In Fig. 3 we have plotted $\sigma(T)$ for a Sn film with $\sigma(300\text{ K}) = 192\ \Omega^{-1}\text{cm}^{-1}$ measured in a perpendicular magnetic field $B = 2.4\text{ T}$. At the lowest temperatures, the $\sigma(T)$ variation is consistent with a $T^{1/2}$ dependence (see dashed line in Fig. 3). A similar $\sigma(T)$ variation was also observed

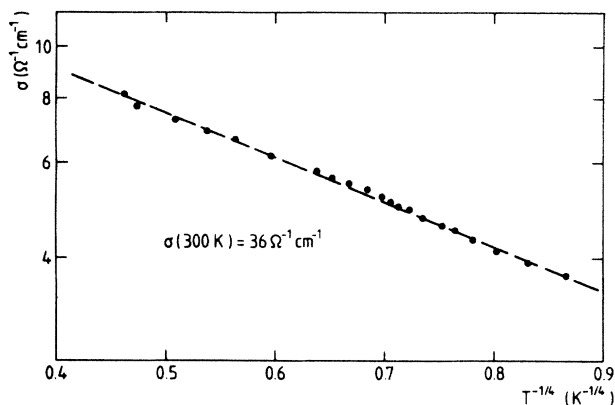


FIG. 2. Conductivity (on a logarithmic scale) as a function of $T^{-1/4}$ for a granular Sn film in the insulating phase, but very near the Anderson transition. The dashed line represents the expected linear behavior for variable range hopping.

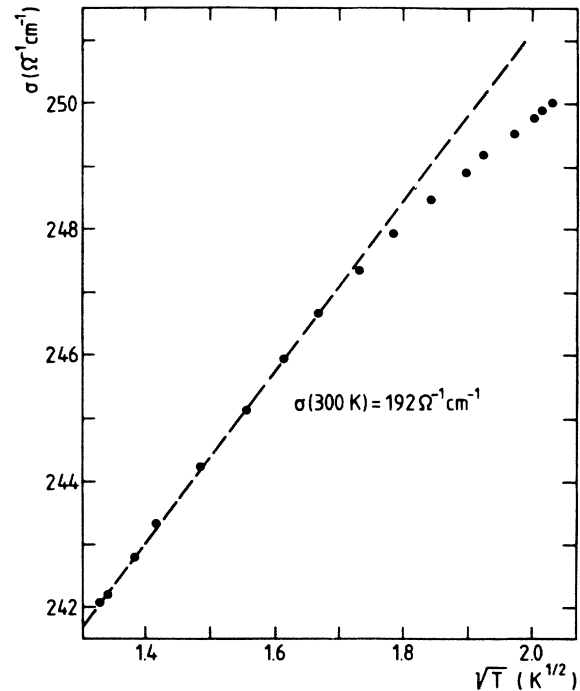


FIG. 3. Variation of the conductivity as a function of $T^{1/2}$ for a granular Sn film in the metallic state. The superconductivity ($T_c = 3.9\text{ K}$) is destroyed by an orthogonal magnetic field $B = 2.4\text{ T}$. The dashed line represents the linear behavior predicted by Eq. (3).

for granular Al films.¹⁰ It is interesting to note that for our metallic granular Sn films the temperature-dependent part of the conductivity in a high magnetic field is nearly independent of the extrapolated value $\sigma(T \rightarrow 0)$. McMillan's scaling result (3) predicts a universal temperature-dependent part of the conductivity for $B = 0\text{ T}$. This prediction was confirmed experimentally for amorphous Nb-Si (Ref. 7) and Au-Ge (Ref. 8) alloys. Although Eq. (3) is no longer valid at high magnetic fields, our experimental results indicate that the Coulomb correlations at high magnetic fields may also give rise to a universal $T^{1/2}$ variation of $\sigma(T)$ at low temperatures.

We discuss briefly also the main features of the anomalous magnetoresistance observed in our Sn films. When the Sn films only contain a small amount of oxygen [$\sigma(300\text{ K}) \geq 10^3\ \Omega^{-1}\text{cm}^{-1}$], they show a highly anisotropic magnetoresistance, typical of a weakly localized two-dimensional superconductor.¹⁸ In an orthogonal magnetic field and at $T > T_c$, there appears a pronounced positive magnetoresistance at very low fields. A detailed analysis of this magnetoresistance indicates that there exists a very strong spin-orbit interaction in our Sn films. A similar result was also found for quench-condensed Sn films containing no oxygen.¹⁹ When the amount of oxygen is increased in our films, the anisotropy of the magnetoresistance is strongly reduced in the normal state ($T > T_c$), and has disappeared almost completely for $\sigma(300\text{ K}) < 200\ \Omega^{-1}\text{cm}^{-1}$. In these three-dimensional Sn films, the magnetoresistance is positive up to $T = 20\text{ K}$ due to the presence of very strong spin-orbit scattering [$C \simeq -0.5$ in Eq. (6)]. This isotropic magnetoresistance can also be partial-

ly explained by the destruction of Coulomb correlations between electrons with opposite spin.²⁰ It is important to note that this positive magnetoresistance persists into the insulating phase. Theoretically,²¹ one expects a negative magnetoresistance, as was observed for insulating granular Al films.¹¹

In the superconducting state, the magnetoresistance remains anisotropic even very close to the Anderson transition. This is probably related to the large superconducting penetration depth of our "dirty" Sn films. It is not clear whether the large negative magnetoresistance which appears in the insulating phase at high magnetic fields for $T \leq 3$ K is related to the possible existence of individual superconducting Sn grains.¹⁴

It is important to note that our magnetoresistance experiments on granular Sn films show that a strong spin-orbit scattering does not destroy superconductivity before the Anderson transition is reached. As indicated in the Introduction, the destruction of superconductivity in Nb-Si mixtures is probably related to a change in the superconducting interaction induced by the alloying.

We also performed electron tunneling measurements in order to observe how the density of states in the granular Sn films changes when the Anderson transition is approached. For a normal Sn electrode, there appears a pronounced square-root anomaly in the density of states as predicted by Eq. (4). This is clearly illustrated in Fig. 4 for a granular Sn film with $\sigma(300\text{ K}) = 149\ \Omega^{-1}\text{ cm}^{-1}$. Since the base electrode of the junction is a pure Sn film

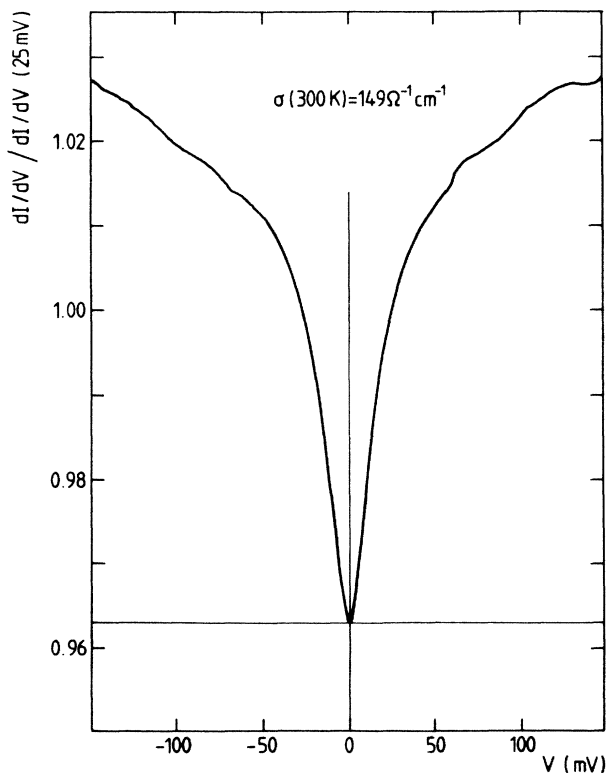


FIG. 4. Normalized derivative of the tunneling current as a function of bias voltage for a junction with a normal granular Sn top electrode [$\sigma(300\text{ K}) = 149\ \Omega^{-1}\text{ cm}^{-1}$]. The base electrode is a pure Sn film which is also in the normal state.

in the normal state, the derivative dI/dV of the tunnel current I as a function of bias voltage V is directly proportional to the density of states $N(|E - E_F| = eV)$ of the granular Sn film. This density of states will, however, be smeared out thermally over an energy interval of the order of $k_B T$.

When we try to fit the result shown in Fig. 4 using Eq. (4), the resulting Δ value is considerably larger than the value estimated from the $\sigma(T)$ variation. The experimentally observed depression of the density of states near the Fermi level is therefore much smaller than the depression we calculate using McMillan's scaling approach. On the other hand, tunneling and conductivity results are in agreement for homogeneous Nb-Si mixtures. The discrepancy which occurs for our granular Sn films can therefore be explained by assuming that the tunneling current is largely determined by tunneling into individual Sn grains. These Sn grains will conserve a perfect metallic behavior even close to the Anderson transition. A similar effect was also observed in granular Pd films.²² It is indeed very likely that the granular structure of our Sn films contains inhomogeneities on a scale which is comparable to the grain size L_g ($L_g \approx 50\ \text{\AA}$ at the Anderson transition, but will be larger when the Sn films are more metallic). Our results indicate that only a small fraction of the tunneling processes occurs on a scale much larger than the length scale L_g [Eq. (4) describes our tunneling results only when $L \gg L_g$].

For a superconducting granular Sn electrode, the tunnel junctions show an additional structure in the derivative dI/dV due to the energy gap in the excitation spectrum of the superconducting state. In Fig. 5 we show dI/dV as a function of V for a junction for which the base electrode is a clean Al film in the normal state. The top electrode is a superconducting Sn film with $\sigma(300\text{ K}) = 135\ \Omega^{-1}\text{ cm}^{-1}$. It is clear that the (temperature-dependent) superconducting gap structure dominates at small bias voltages ($V < 3$ meV). At higher bias voltages ($V > 5$ meV), the square-root anomaly described by Eq. (4) dominates and is nearly independent of temperature since $k_B T \ll \Delta$. As for the tunneling results shown in Fig. 4, we calculate a Δ value that is much smaller than what could be expected from the $\sigma(T)$ variation.

A detailed analysis of the superconducting gap structure for the granular Sn film shows that in the vicinity of the Anderson transition, the value of the superconducting gap is approximately the same as for a pure Sn film (≈ 0.57 meV). We observe only a broadening of the energy-gap edge. This occurs simultaneously with the broadening of the superconducting transition (see inset of Fig. 1). The increasing width of the superconducting transition in granular superconductors can be explained by the critical fluctuations in the individual metallic grains that become more and more isolated.¹⁷ Our experimental results indicate that the superconducting as well as the normal tunneling mainly probe the allowed energy states in the Sn grains. In this way we can explain why the destruction of the superconductivity on a macroscopic length scale (depression of T_c in the inset of Fig. 1) is not reflected by the superconducting tunneling measurements (the energy gap remains constant when the Anderson

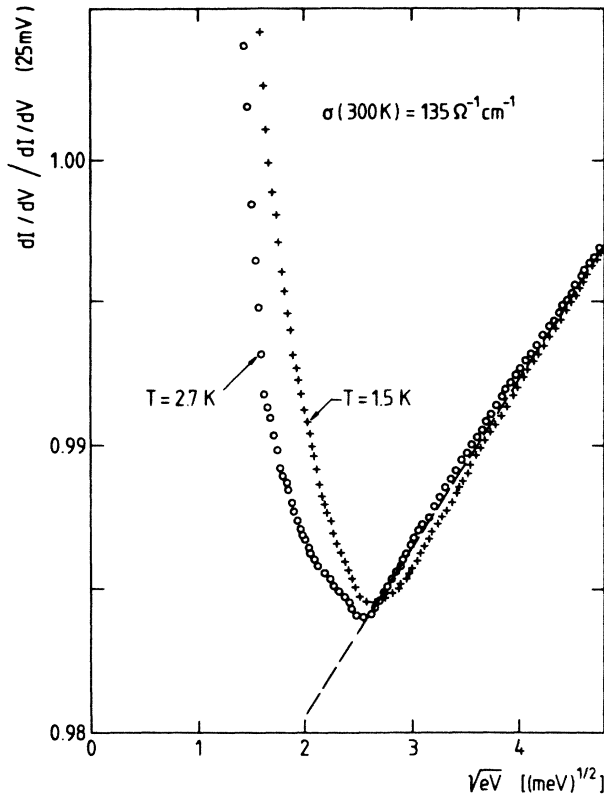


FIG. 5. Normalized derivative of the tunneling current as a function of the square root of the electron energy eV for a junction with a superconducting ($T_c = 3.0$ K) granular Sn top electrode [$\sigma(300 \text{ K}) = 135 \Omega^{-1} \text{ cm}^{-1}$]. The base electrode of the junction is a normal Al film. The dashed line represents the linear behavior predicted by Eq. (4).

transition is approached). Recently, considerable energy-gap edge broadening was also reported for granular Al films,²³ but it was explained as a lifetime effect due to the divergence of the inelastic scattering rate near the Anderson transition.

Concerning the analysis of our tunneling data, one could also argue that the large Δ values obtained from Eq. (4) are due to the significant voltage drop which develops across the granular Sn film in the tunneling window. However, using a simple theoretical model,²⁴ we can estimate that the finite resistance of the granular Sn film will not alter the conclusions drawn from the result shown in Fig. 4. Moreover, when the granular Sn film becomes superconducting (see Fig. 5), we still observe a much too large Δ value.

When the granular Sn films are insulating [$\sigma(300 \text{ K}) < 40 \Omega^{-1} \text{ cm}^{-1}$], dI/dV becomes a parabolic function of V . A similar effect was also reported for amorphous Au-Ge mixtures.²⁵ The parabolic shape is probably related to the opening of a correlation gap in the insulating phase. Due to the appreciable charging effects in the insulating electrode, the tunneling results can no longer be linked directly to the density of states of the insulator. The correlation gap will influence the thermally activated conduction process at low enough temperatures as predicted by Efros and Shklovskii.²⁶ This is indeed observed as shown in Fig. 6 for a Sn film with $\sigma(300$

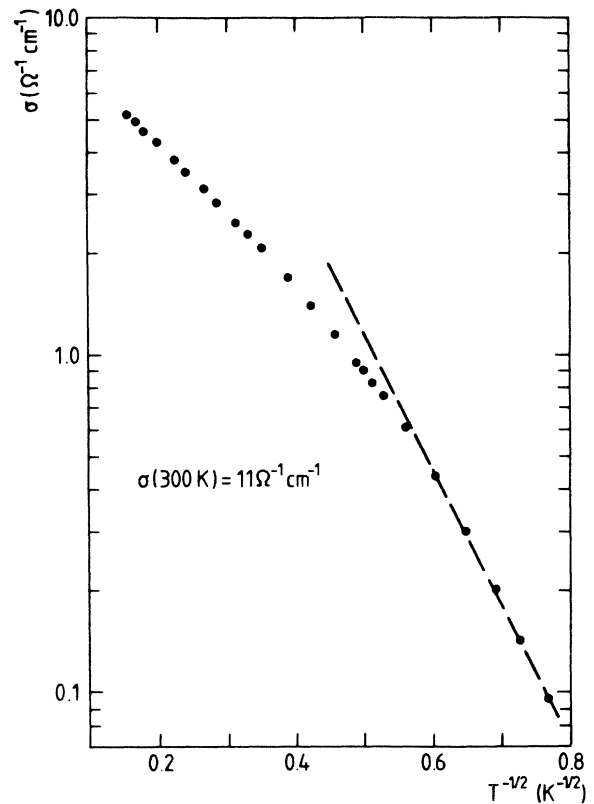


FIG. 6. Conductivity (on a logarithmic scale) as a function of $T^{-1/2}$ for a granular Sn film in the insulating phase far from the Anderson transition. The dashed line represents the expected linear behavior for variable range hopping in the presence of a correlation gap.

$\text{K}) = 11 \Omega^{-1} \text{ cm}^{-1}$. At the lowest temperatures ($1.5 < T < 4 \text{ K}$) $\ln(\sigma) \propto T^{-1/2}$, as is expected for variable range hopping in the presence of a large correlation gap. At higher temperatures, $\ln(\sigma) \propto T^{-1/4}$. A similar transition from $\ln(\sigma) \propto T^{-1/4}$ towards $\ln(\sigma) \propto T^{-1/2}$ does not appear for the Sn film shown in Fig. 2. Since this film was very close to the Anderson transition (very small correlation gap), the $T^{-1/2}$ dependence will only show up at very low temperatures ($T \ll 1 \text{ K}$).

IV. CONCLUSIONS

From conductivity measurements as a function of temperature and magnetic field, we were able to show that the disappearance of the metallic behavior in granular Sn films is governed by an Anderson transition. Due to the granular structure which is inhomogeneous on an atomic length scale, the critical conductivity σ_c is as low as $40 \Omega^{-1} \text{ cm}^{-1}$. Superconductivity and normal metallic behavior disappear simultaneously on a macroscopic scale at the metal-insulator transition. As predicted by the scaling theory for the Anderson transition, the disorder influences the conductivity already in the metallic regime. However, the inhomogeneous granular structure and the presence of the superconductivity do not allow a quantitative comparison with the theoretical models.

Tunneling measurements performed on granular Sn films indicated that the tunneling current in the metallic regime is mainly determined by the local normal and su-

perconducting properties of the grains. The influence of the Coulomb interaction on the Anderson transition is confirmed by the appearance of a square-root anomaly in the density of states around the Fermi level. Due to the inhomogeneous, granular structure, the depression of the density of states near the Fermi level is, however, considerably smaller than for a homogeneous amorphous metal. The granular structure also causes a significant broadening of the superconducting energy-gap edge.

ACKNOWLEDGMENTS

We thank G. Deutscher, Y. Imry, P. Lindenfeld, G. Thomas, and P. Santhanam for enlightening discussions, and C. Creemers (Physical-Chemical Laboratory, K. U. Leuven) for the ISS measurements. We express our gratitude to the Belgian Interuniversitair Instituut voor Kernwetenschappen for financial support.

*Present address: IBM Thomas J. Watson Research Center, Yorktown Heights, NY 10598.

¹N. F. Mott, *Metal-Insulator Transitions* (Taylor and Francis, London, 1974).

²G. A. Thomas and M. A. Paalanen, *Localization, Interaction and Transport Phenomena in Impure Metals*, edited by G. Bergmann, Y. Bruynseraede, and B. Kramer (Springer, Heidelberg, 1985).

³E. Abrahams, P. W. Anderson, D. C. Licciardello, and T. V. Ramakrishnan, *Phys. Rev. Lett.* **42**, 673 (1979).

⁴B. L. Altshuler, A. G. Aronov, and P. A. Lee, *Phys. Rev. Lett.* **44**, 1288 (1980).

⁵P. W. Anderson, *Phys. Rev.* **109**, 1492 (1958).

⁶W. L. McMillan, *Phys. Rev. B* **24**, 2739 (1981).

⁷G. Hertel, D. J. Bishop, E. G. Spencer, J. M. Rowell, and R. C. Dynes, *Phys. Rev. Lett.* **50**, 743 (1983).

⁸B. W. Dodson, W. L. McMillan, J. M. Mochel, and R. C. Dynes, *Phys. Rev. Lett.* **46**, 46 (1981).

⁹R. C. Dynes and J. P. Garno, *Phys. Rev. Lett.* **46**, 137 (1981).

¹⁰T. Chui, G. Deutscher, P. Lindenfeld, and W. L. McLean, *Phys. Rev. B* **23**, 6172 (1981).

¹¹H. K. Sin, P. Lindenfeld, and W. L. McLean, *Phys. Rev. B* **30**, 2951 (1984).

¹²Y. Imry, *Phys. Rev. B* **24**, 1107 (1984).

¹³B. Abeles and P. Sheng, in *Electrical Transport and Optical Properties of Inhomogeneous Media*, edited by J. C. Garland

and D. B. Tanner (AIP, New York, 1978).

¹⁴G. Deutscher, M. Palevski, and R. Rosenbaum, in *Localization, Interaction and Transport Phenomena in Impure Metals*, edited by G. Bergmann, Y. Bruynseraede, and B. Kramer (Springer, Heidelberg, 1985).

¹⁵Y. Imry and M. Strongin, *Phys. Rev. B* **24**, 6353 (1981).

¹⁶S. Akselrod, M. Pasternak, and S. Bukshpan, *J. Low Temp. Phys.* **17**, 375 (1974).

¹⁷G. Deutscher, H. Fenichel, M. Gershenson, E. Grunbaum, and Z. Ovadyahu, *J. Low Temp. Phys.* **10**, 231 (1973).

¹⁸Y. Bruynseraede, M. Gijs, C. Van Haesendonck, and G. Deutscher, *Phys. Rev. Lett.* **50**, 277 (1983).

¹⁹G. Bergmann, *Phys. Rev. B* **29**, 6114 (1984).

²⁰P. A. Lee and T. V. Ramakrishnan, *Phys. Rev. B* **26**, 4009 (1982).

²¹B. L. Altshuler and A. G. Aronov, *Pis'ma Zh. Eksp. Teor. Fiz.* **37**, 145 (1983) [*JETP Lett.* **37**, 175 (1983)].

²²S. Weng, S. Moehlecke, M. Strongin, and A. Zangwill, *Phys. Rev. Lett.* **50**, 1795 (1983).

²³R. C. Dynes, J. P. Garno, G. B. Hertel, and T. P. Orlando, *Phys. Rev. Lett.* **53**, 2437 (1984).

²⁴J. W. Osmun, *Phys. Rev. B* **21**, 2829 (1980).

²⁵W. L. McMillan and J. M. Mochel, *Phys. Rev. Lett.* **46**, 556 (1981).

²⁶A. L. Efros and B. I. Shklovskii, *J. Phys. C* **8**, L49 (1975).